

Advantages of Capacitive Micromachined Ultrasonics Transducers (CMUTs) for High Intensity Focused Ultrasound (HIFU)

Serena H. Wong*, Mario Kupnik*, Kim Butts-Pauly†, and Butrus T. Khuri-Yakub*

*Edward L. Ginzton Laboratory, Stanford University, Stanford, CA

†Department of Radiology, Stanford University, Stanford, CA 94305

Email: shwong@stanford.edu and khuriyakub@stanford.edu

Abstract—In the past ten years, high intensity focused ultrasound (HIFU) has become popular for minimally invasive and non-invasive therapies. Traditionally piezoelectric transducers have been used for HIFU applications, but capacitive micromachined ultrasonic transducers (CMUTs) have been shown to have advantages, including ease of fabrication and efficient performance. In this paper, we show the fabrication and testing of CMUTs specifically designed for HIFU. We compare the operation of these designs with finite element models. In addition, we demonstrate that CMUTs can operate under high pressure and continuous wave (CW) conditions, with minimal self-heating, a problem that piezoelectric transducers often face. Finally, we demonstrate MR-temperature monitoring of the heating created by an unfocused HIFU CMUT.

I. INTRODUCTION

High intensity focused ultrasound (HIFU) has become popular in minimally invasive and noninvasive applications because it can be applied at a distance without damage to intervening tissue. Such applications include ablation of electrical pathways in the heart to prevent cardiac arrhythmias and destruction of diseased tissues, like cancers. Our goal is to develop a hand-held transducer to treat lower abdominal cancers. These CMUT arrays will be guided by MR-temperature maps that can monitor lesion formation and tissue necrosis in real-time.

Traditionally, piezoelectric transducers have been used for HIFU applications, but capacitive micromachined ultrasound transducers (CMUTs) have demonstrated many advantages including ease of fabrication, integration with electronics, and competitive bandwidth and high power performance [1], [2]. Silicon micro-machining methods enable fabrication of membrane shapes and geometries [3], [4], [5] and allow tailoring of membrane properties used to optimize performance. Most importantly, CMUTs can be constructed with a conductive silicon membrane as a top electrode, removing the need for metal on the surface of the cells. Removal of this metal is advantageous because it eliminates electromigration problems, which are caused by high currents in high-power, CW operation. Also, the silicon itself is highly thermally conductive, which reduces self-heating, a problem that piezoelectric ultrasonic transducers often face [6], [7]. Furthermore, these silicon membranes and the oxide cavities are entirely MR compatible [8].

Last year, we presented the design and simulation of cells

TABLE I
DIMENSIONS OF THE CELLS.

parameter	design 1	design 2
membrane thickness (tm)	6 μm	6 μm
radius (rm)	60 μm	70 μm
gap	0.4 μm	0.4 μm
insulation thickness (ti)	0.57 μm	0.57 μm

and transducer configurations for non-invasive cancer therapy of lower abdominal cancers [9]. In this paper, we show the fabrication and operation of these cells and compare them to the finite element models used for design. We also demonstrate MR-temperature monitoring of a heated spot created by an unfocused HIFU CMUT.

II. METHODS

Finite element models (ANSYS, Canonsburg, PA) were used to simulate and design cells for HIFU. These models were described in detail in a previous conference paper [9]. The cells we designed were then fabricated using the direct-fusion, wafer bonding process. The harmonic and dynamic response in immersion was tested and compared to the finite element models used for design before experiments with CW operation and MR-guidance.

A. CMUT Fabrication

CMUTs (Fig. 1) were fabricated using a direct wafer bonding process. In this process, two successive oxidations of a prime wafer formed the cavity and insulation layer of the membrane. A silicon-on-insulator wafer (SOI) with active layer of the desired thickness was then wafer-bonded to the wafer with cavities. After the handle wafer and buried oxide layer were removed, the electrical contacts were formed and the transducer elements were defined [10].

The fabricated cells had thick membranes, wide radiuses, and relatively large gap heights to achieve center frequencies in the range of 1-5 MHz and output pressures of 1-2 MPa peak to peak. In particular we use two designs for experiments in this paper (Table I).

B. Experimental Methods

We measured the static and dynamic responses and compared them to simulation. We mounted the test transducers on

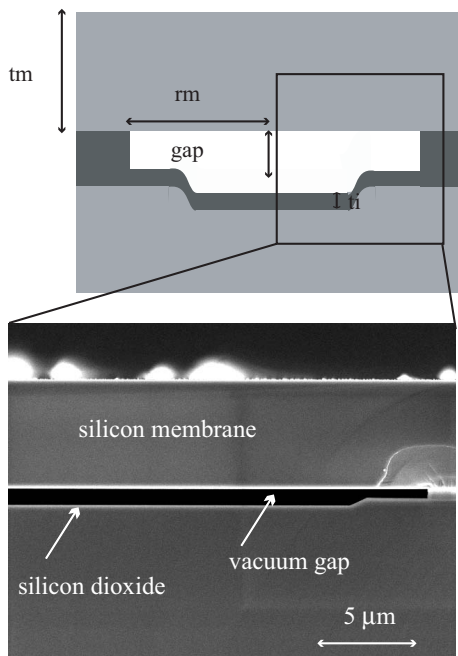


Fig. 1. SEM pictures of CMUT design.

a printed circuit board using silver epoxy. Gold wire bonds were used to connect the pads on the device with the printed circuit board traces.

Collapse voltage and static deflection were measured in air by applying DC voltage (PS310, Stanford Reserch Systems, Stanford, CA) and measuring the resulting deflection using a white light interferometer (NewView 2000, Zygo Corporation, Sunnyvale, CA).

For dynamic response measurements, the CMUTs were immersed in a tank filled with soybean oil (Fig. 2). Oil provides electrical insulation, has acoustic properties that are very similar to liver tissue [1], and has higher thermal insulation properties than water. A PZT_Z44_0400 hydrophone (Onda Corporation, Sunnyvale, CA) was positioned 2 cm from the surface to measure the output pressure. The measurement data was corrected for the frequency response [11] of the hydrophone and sound attenuation and diffraction [12] to calculate the pressure at the surface of the transducer. In addition, a fluoroptic temperature fiber (Luxtron Corporation, Santa Clara, CA) was placed in direct contact with the surface of the CMUT to measure the degree of self-heating. Compared to thermocouples, the fluoroptic temperature sensor (Lumasense Technologies, Sunnyvale, CA) is an optical based temperature measurement device, which eliminates the danger of causing an electrical short circuit on the CMUT.

To obtain the harmonic response, we biased the CMUT at 80% of collapse and applied a 16 Vpp, 20 MHz square pulse. By taking the Fourier transform of the hydrophone measurement and accounting for the frequency dependence of the hydrophone as well as attenuation and diffraction [12],

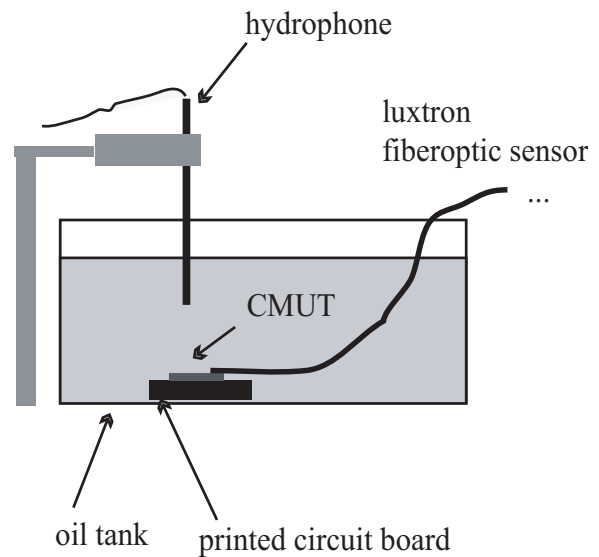


Fig. 2. Diagrams of the setup used for immersion testing.

we calculated the frequency response of the transducer. For dynamic response, DC biases from 60-80% of the collapse voltage were superimposed on a 2.5 MHz, 30 cycle burst with amplitudes from 0-300 Vpp. We accounted for attenuation and diffraction to back-calculate the output pressure at the surface of the CMUT from the hydrophone measurements. From CW measurements, we chose a DC voltage that was 80% of the collapse voltage and an AC voltage of 250 Vpp to produce a surface output pressure of 1.7 MPa peak to peak, or 20 W/cm². The CMUT was operated with a CW sine input for an hour, and the temperature rise at the surface, measured by the fiberoptic temperature sensors, was evaluated.

Finally, we monitored heating from CW operation of a test transducer using a 3.0 T MRI scanner (Lucas Center, Stanford, CA). We placed the CMUT on the bench top and isolated it electrically from the gel phantom by covering it with a couple of drops of soybean oil and a sheet of polyethylene. An ultrasonic gel (MediChoice, Mechanicsville, VA) was then used to couple sound into the HIFU phantom (Insightec, Haifu, Israel). The temperature was measured in this gel in the sagittal plane cutting through the transducer (Fig. 3). The CMUT, which was matched to 50 ohms with a large air-core inductor, was operated in CW mode for 5 min. The temperature in the phantom was measured using a fast gradient echo sequence with TR/TE (Repetition Time/Echo Time) of 28.7/19.1 seconds; one hundred images were captured over a 12 min time period.

Temperature change was detected by a shift in the proton resonance frequency and a resulting change in phase, $\Delta\phi$. We calculated this phase changes by subtracting the phase images of successive frames. The temperature change, ΔT , was calculated by:

$$\Delta T = \frac{\Delta\phi}{\alpha 2\pi\gamma B_0 T E}, \quad (1)$$

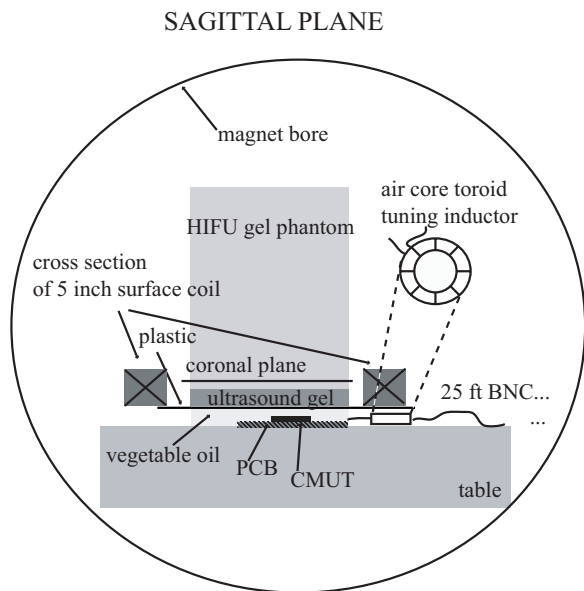


Fig. 3. Diagrams of the setup used for testing inside the MRI magnet.

TABLE II
COMPARISON OF COLLAPSE VOLTAGE.

design	measured	simulated	error
1	293 V	275 V	-6.5%
2	208 V	211 V	-1.4%

where the proton resonance shift α is 0.01 ppm/ $^{\circ}$ C, the proton resonance frequency γ is 26734 rad/sec/G, the magnetic field strength B_0 is 3.0 T, and transmit echo time (TE) is 19.1 seconds [13], [14].

C. Results and Discussion

The fabricated designs showed good agreement to the finite element models used for design [9]. The collapse voltage matched with 7% (Table II). The center frequency in immersion also matched within 20% of the model. A comparison of the measured and simulated harmonic response of design 2 shows very similar center frequency and bandwidth (Fig. 4).

The maximum acoustic output pressure achieved from both designs was less than the expected output pressures calculated in the finite element models. Charging effects in the silicon dioxide, acoustic cross talk, and parasitic capacitance account for the lost pressure. We calculate the amount of charging by measuring curves of pressure with varying DC bias voltage. The voltage shift of successive sweeps in DC voltage showed a shift of 30 V for the membrane configuration in design 2. If we accounted for 30 V in our model, we found the results matched fairly well (Fig. 5).

Taking design 2, we examined the operation and temperature rises of the CMUT devices under CW operation with a DC voltage 80% of collapse voltage and a CW AC voltage of 250 V_{pp} at 2.5 MHz. We measured an output pressure of 1.7 MPa peak to peak (20 W/cm²) over one hour continuously. The fiberoptic temperature sensor placed at the surface of the

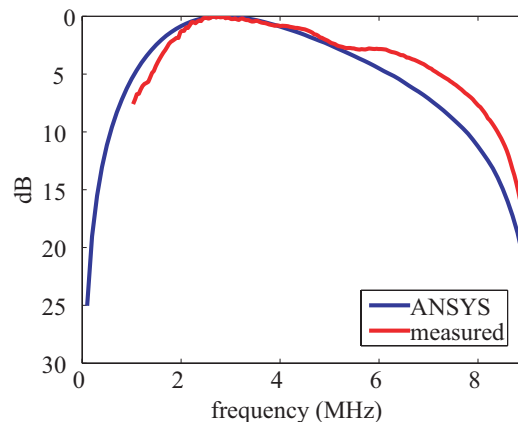


Fig. 4. Measured and simulated harmonic response of design 2.

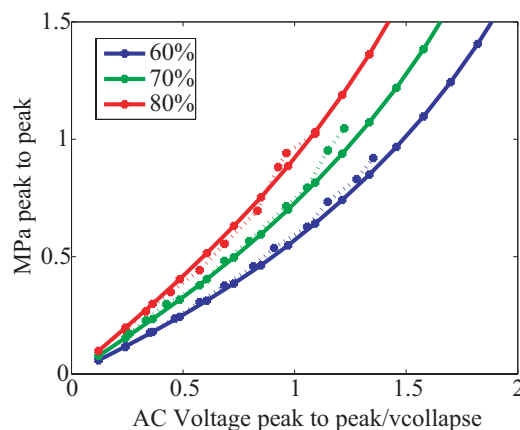


Fig. 5. Comparison of measured (dotted lines) and simulated (solid lines) output pressure. 30 V of charging was incorporated into the simulation model.

CMUT showed no more than a 10 degree rise in this time period, which suggests that self-heating is minimal (Fig. 6). Given that the thermal conductivity of oil is much less than that of water, the CMUT temperature rise should be even less when used in water applications.

After demonstrating stable CW operation with minimal self-heating, we used an unfocused HIFU CMUT (design 1) to heat a HIFU phantom and monitored the temperature rise in the 3.0 T MRI scanner. We found that the transducer was 68% efficient and the phantom reached a maximum temperature change of 16 $^{\circ}$ C over 5 min (Fig. 7), which is adequate for HIFU applications [15].

III. CONCLUSION

CMUTs designed for non-invasive HIFU have been fabricated and tested. These CMUTs were designed using finite element analysis and had good agreement with the models. We have shown that CMUTs can operate in CW operation with output pressures of 1.7 MPa (20 W/cm²) with minimal self-heating (less than 10 $^{\circ}$ C). This is advantageous because

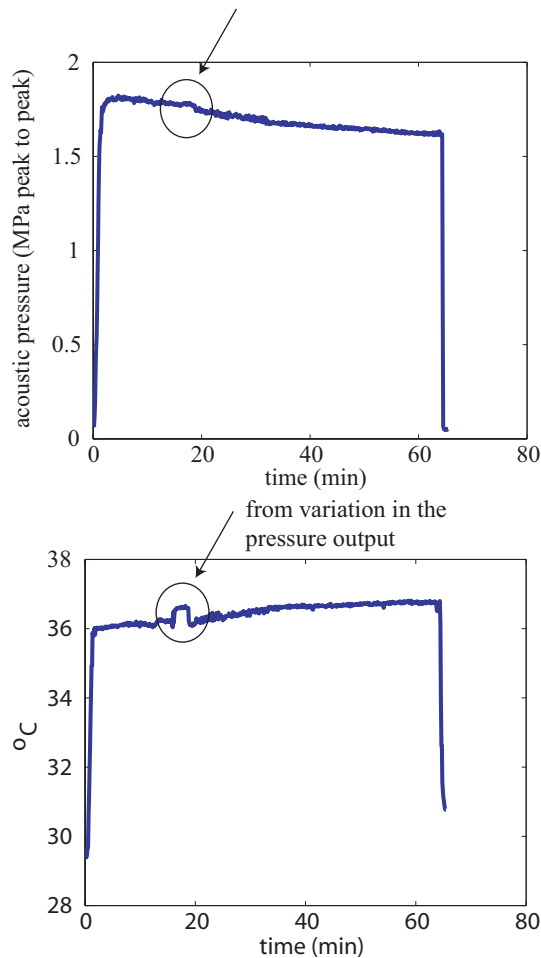


Fig. 6. CW acoustic pressure (top) and CMUT surface temperature (bottom) measured over a HIFU treatment course of 1 hour. Note that the jump in temperature (circled with the arrow) corresponds to a jump in pressure.

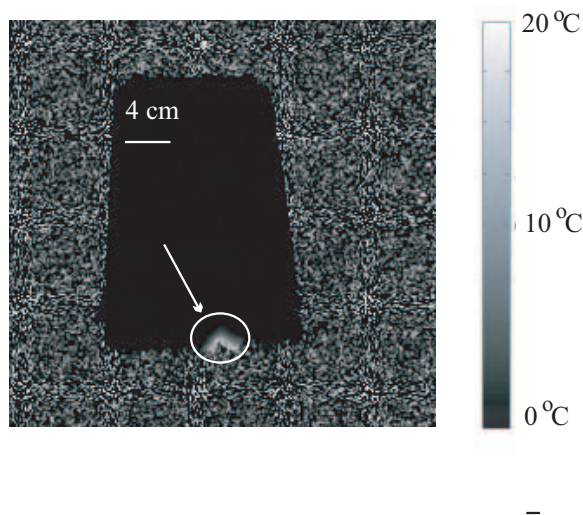


Fig. 7. MRI temperature map of the heat distribution in a HIFU gel phantom after 5 min of CW heating by an unfocused CMUT.

it will reduce undesirable near-field heating in minimally invasive and non-invasive applications. Finally, we have shown significant heating of phantom using an unfocused CMUT transducer and demonstrated MR-temperature mapping of a CMUT.

In the future, we plan to improve our models by taking into account thermal processing effects to better understand the initial stress state of the membranes. This will enable us to better design cells that can provide even more efficient and greater output pressures at lower voltages for use in HIFU applications. With these promising preliminary results, we also plan to fabricate annular ring arrays for focused ultrasound. With this focused transducer, even faster and larger temperature rises could be realized than the transducer used for our current experiments.

ACKNOWLEDGMENT

This research was supported under NIH R01 CA77677, R01 CA 121163

REFERENCES

- [1] O. Oralkan, A.S. Ergun, C. Cheng, J.A. Johnson, M. Karaman, T. Lee, B.T. Khuri-Yakub, "Volumetric Ultrasound Imaging Using 2-D CMUT Arrays," *IEEE Transactions on Ultrasonics*, 50(11), pp. 1581-1594.
- [2] D.M. Mills and L.S. Smith, "Real Time In-vivo with Capacitive Micromachined Ultrasound Transducer (cMUT) Linear Arrays," in *Proceedings of IEEE Ultrason. Symp.*, 2003, pp.568-571.
- [3] Y. Huang, E.O. Haeggstrom, X. Zhuang, A.S. Ergun, and B.T. Khuri-Yakub, "Capacitive micromachined ultrasonics transducers (CMUTs) with piston-shaped membranes," in *Proceeding of the IEEE Ultrason. Symposium*, 2006, pp.598-592.
- [4] Y. Huang, E.O. Haeggstrom, X. Zhuang, A.S. Ergun, and B.T. Khuri-Yakub, "Optimized Membrane Configuration Improves CMUT Performance", *Proceedings of the IEEE Ultrasonics Symposium 2004*, pp.505-508.
- [5] P.J. French and P.M. Sarro, "Surface versus bulk micromachining: the conest for suitable applications," *Journal of Micromechanical Micro-engineering*, 8, pp.45-53.
- [6] Y. Chen, Y. Wen, and P. Lai, "Loss Mechanisms in Piezoelectric Transducer and Its Response to Stress," *Proceedings of the IEEE Information Acquisition*, 2004, pp.213-219.
- [7] <http://www.npl.co.uk/materials/functional/temperature/index.html>.
- [8] J.F. Schenck, "The role of magnetic susceptibility in magnetic resonance imaging: MRI magnetic compatibility of the first and second kinds", *Medical Physics*, 1996:23(6)
- [9] S.H. Wong, A.S. Ergun, G. Yaralioglu, M. Kupnik, X. Zhuang, O. Oralkan, "Capacitive Micromachined Ultrasonic Transducers for High Intensity Focused Ablation of Upper Abdominal Tumors," in *Proceedings of the Ultrasonics Symposium*, pp.841-844.
- [10] Huang, Y.L., et al., "Fabricating capacitive micromachined ultrasonic transducers with wafer-bonding technology", *Journal of Microelectromechanical Systems*, 12(2), pp. 128-137.
- [11] <http://www.ondacorp.com>
- [12] G. Kino, *Acoustics Waves: Devices, Imaging, and Analog Signal Processing*, Englewood Cliffs, New Jersey: Prentice-Hall, 1987.
- [13] V. Rieke, K.K. Vigen, G. Sommer, B.L. Daniel, J.M. Pauly, and K. Butts, "Referenceless PRF shift thermometry", *Magnetic Resonance in Medicine*, 51(6), pp.1223-1231.
- [14] H.E. Cline, J.F. Schenck, K. Hynynen, R.D. Watkins, S.P. Souza, and F.A. Jolesz, "MR-guided focused ultrasound surgery", *Journal of Computer Assisted Tomography*, 16, pp. 956-965.
- [15] S.H. Wong, R.D. Watkins, M. Kupnik, K. Butts-Pauly, and B.T. Khuri-Yakub, "MR-guided temperature maps of HIFU CMUT", submitted for publication.